HIGH VOLTAGE TECHNOLOGY

A. S. Denholm

Ion Physics Corporation
Burlington, Massachusetts

Summary

Vacuum, high pressure gases and solid dielectrics, which are used extensively for the insulation of high voltages in particle accelerators, are discussed. Examples are given of high voltage technology applied to the acceleration of micron size particles and to the production of intense pulses of radiation of nanosecond duration.

1. Introduction

Particle accelerators can be placed in two general classes; those which operate by direct electrostatic acceleration and those which use time varying electric or magnetic fields. The following discussion will relate primarily to the direct acceleration machine, where the maximum particle energy is determined by the voltage which can be insulated.

For obvious reasons the acceleration of particles to high energy has to be accomplished in a vacuum, and fortunately below about 10^{-3} torr, where mean free paths are of the order of system dimensions, the vacuum dielectric has good insulating properties; although occasionally proving intransigent. The usual complimentary insulating media are high pressure gas and solid dielectric; the solid dielectric forming the boundary between vacuum and gas. Solid dielectrics such as glass, alumina, and Lucite can support much higher fields than either the vacuum or high pressure gas, particularly if voids are eliminated and care is taken to use a relatively uniform field geometry. Fig. 1 presents data on solid dielectrics which are of specific interest to an accelerator designer. This information was assembled from an article by Charpentier,[1] which also describes the technique used to obtain such high stresses at relatively large gaps. Thin films of solid dielectric support direct fields of several megavolts per as shown by the data on Table 1.[2] Solid trics are taxed close to the limit of their strength in energy storage devices; and acting factors involving voltage reversal, in voids, and lifetime have to be deter-

2. Insulation in Vacuum

In studying the available information on electric breakdown in vacuum, it is useful to group the studies into two classes; those done with superior vacuum conditions (say less than 10^{-7} torr), and the rest. Above 10^{-7} torr electrodes are likely to be contaminated and below 10^{-7} torr if suitably treated they may be uncontaminated.

When a sufficiently high electric field is applied to a negative surface, electrons can be extracted by the field emission process. The law which governs this emission was originally determined by Fowler and Nordheim,[3] and gives to a good approximation, a linear relationship between $\ln J/E^2$ vs. $1/E$, where J is current density and E is electric field. This is usually plotted as $\ln I/V^2$ vs. $1/V$, since the current I is taken to come from a constant area emitter and the voltage V is proportional to E. To account for the emission which is found with large area electrodes, it is necessary to invoke an enhancement factor (γ), such that the true field at a microprojection on the cathode is γE, or $\gamma V/d$ for a parallel plane gap. Fig. 2 shows a Fowler-Nordheim plot for a stainless steel needle with a 2μ tip at 2×10^{-6} torr together with the reduced field emission obtained at 2×10^{-5} torr. This reduced emission is apparently caused by bombardment and reduction by sputtering of whiskers on the tip by positive ions produced close to the tip in the residual gas.[4]

The most significant basic studies in recent years on breakdown in vacuum are those undertaken at the University of Illinois.[5,6] The results of these studies, which relate to vacuum conditions at 2×10^{-9} torr or less, led to a "physical picture which quantitatively related predischarge characteristics to the initiative process, together with supporting experimental evidence for this interpretation of the initiating process." Experimental data obtained at the University of Illinois, and elsewhere under superior vacuum conditions,[7,8] were suitably treated to show that breakdown takes place at a critical field at microscopic points or whiskers on the cathode surface; for tungsten 6.5×10^{7} V/cm. Breakdown occurs because of current density effects at these projections, and "field emission

from these points can be used as a tool to ascertain the field enhancement (and hence the approximate geometry) due to such whiskers in a nondestructive manner, and thus to predict the voltage at which the breakdown will next occur."

It has been noted that when vacuum break-down takes place across small gaps, for example 1 mm, that discharge marks are often centered on carbide or sulfide inclusions in the metal. This led to a study of the influences of electrode metallurgy on vacuum breakdown, particularly on metals with a minimum of inclusions. In this investigation the best electrode metal was found to be a titanium alloy (Ti-7Al-4Mo) which is vacuum melted during production and relatively free of inclusions. Voltages above 100 kV direct were supported across 1 mm gaps. This information which was obtained by McCoy and Thayer[9] led other investigators to study titanium and its alloys with considerable success.[10]

Unfortunately, relatively poor vacuum ($>10^{-7}$ torr) and contaminated surfaces are usual in accelerator systems, a situation conducive to microdischarges. These discharges, which tend to be dependent on contamination rather than electrode material and typical of gaps above about 1 mm, are small pulses of charge which start to cross a vacuum gap at a particular threshold voltage (Fig. 3a).[11] The pulse charge, repetition frequency, and duration, depend on the electrode surface area, the supply impedance, and the degree of contamination of the electrodes.[11-14] The threshold voltage can vary over a wide range as shown in Fig. 4, which is from data given by Arnal.[12] It can be seen from this figure that microdischarge effects can be expected in accelerator tubes; and this has been demonstrated by Mansfield and Fortescue[11](Fig. 3b). It appears that the current loading phenomenon which limits the total voltage performance of tubes[15] is related to the microdischarge effect. Both the threshold voltage for microdischarges and the total voltage performance of an accelerator tube, or high vacuum bushing,[16] can be raised, by increasing the residual pressure to about 2×10^{-4} torr. This improvement apparently results from residual gas atoms interfering with the passage of charged particles across the gap.

It has been shown[12,17] that the initiation of microdischarges is a cascade process involving secondary ionization at the electrode surfaces. The ions involved are hydrogen, and a pulse occurs when

$$A \times B > 1$$

where A is the number of H^+ ions emitted per H^- ion bombarding the anode surface,

and B is the number of H^- ions emitted per H^+ion bombarding the cathode surface.

Mansfield[17] has demonstrated that this product AB is close to 1. Although the initiation process is ionic, it has been shown[18] that most of the charge flow is electronic; which must be related to the secondary emission coefficient of ions for electrons and of electrons for ions on contaminated surfaces.

It is difficult to obtain large particle accelerators, or velocity separators, free of the type of contamination which leads to microdischarges (current loading), and this is emphasized by the data given in Table 2. This information was supplied by Ennos[19], and shows the thickness of a carbonaceous layer laid down by an electron beam because of a source of contamination elsewhere in the vacuum system.

An attractive approach to reducing current loading and hence improving the total voltage performance of accelerators is that of the inclined field tube.[20] In this tube, unwanted secondary particles are swept into the walls before they reach significant energies. This technique can be very effective, as shown in Fig. 5, but some sophistication in design is needed to ensure that the wanted particles which are being accelerated can undulate successfully through the tube.

The insulating properties of vacuum gaps at small spacings[21] and at large spacings[22,23] can be improved by the application of a suitable dielectric film to the cathode surface. With small spacings of the order 1 mm, gaps with dielectric coatings have not yet been able to exceed the voltage which can be supported by the best metal surfaced electrodes as far as small areas are concerned (20 cm^2- 100 kV/mm), but they have for large areas (1000 cm^2) where the best performance of all-metal electrodes is relatively poor ($\sim$ 30 kV/mm).

High voltages cannot be applied in vacuum without the use of solid dielectrics for support, and for an equal spacing, solid dielectric flashover occurs at a lower gradient than breakdown through the vacuum gap. This problem has been studied by various investigators,[24-26] with the conclusion that termination conditions are most important, particularly at the negative end of the dielectric, where intimate contact should be obtained at the parting of the solid dielectric and

metal surfaces. A plot of insulation strength (10 minute withstand) for alumina ceramic is given in Fig. 6. Shannon, et al[26] have shown that 80 kV / cm can be attained across glass surfaces with geometries suitable for accelerator tube con - struction.

At the beginning of this section an arbitrary pressure of 10^{-7} torr was given as a rough indi- cation of studies which were made in contami - nated situations. Having discussed the micro - discharge phenomenon, a better guide to surface condition is the existence of ion initiated micro- discharges at gaps of millimeters or more. Sur- faces can be cleaned by heating in vacuum, but too much enthusiasm in this respect (e. g., 900°C for nickel)[27] will produce whiskers, which lead to breakdown at relatively low macroscopic gradients.

3. Insulation in High Pressure Gas

When a sufficiently high electric field is ap- plied to a gas, avalanche ionization (Townsend α process) occurs which will lead to breakdown. The final stages of spark development will not be dis- cussed here, and it is sufficient to note that elec- tron emitting processes at the cathode surface can influence breakdown voltage, which consequently becomes strongly material dependent at high gas pressures. Trump, et al[28] show, for example, the spark-over gradient at 400 psig to be about 50% higher for stainless steel electrodes than for aluminum. Although some low level conditioning sparks occur in a high pressure gas, it is a much more reliable medium than high vacuum and main- tains its high electric field strength at large gaps.

Mixtures of N_2, CO_2 and SF_6 are used exten- sively in electrostatic accelerators. Philp[29] studied pure SF_6 and equal part mixtures of N_2 and CO_2 to voltages above 2 MV, and showed that gradients of more than 100 MV/m can be insulated on a 19 mm diameter electrode in 20 atmospheres of SF_6. Figure 7, which is from Philp's data, shows the maximum gradient withstood for three minutes without breakdown.

The higher dielectric strength of SF_6 with regard to a simple gas such as N_2 is due largely to its electro-negative properties; i. e., the ability to attach electrons to make negative ions. Carbon dioxide, although not as good as SF_6, is superior to N_2 for the same reason. Sulfur hexafluoride is an expensive gas, which can make its use unattrac- tive for large machines. Fortunately, the addition of a small fraction of SF_6 to N_2 gives breakdown values relatively close to that of pure SF_6 as shown in Fig. 8.[30,31]

Sulfur hexafluoride is an inert, non-toxic gas, but if subjected to energetic sparking it breaks down into components which are corrosive and highly toxic. One of the products, disulfur dexa- fluoride, S_2F_{10}, is an agent used in chemical war- fare research. Processes are available for con- tinuously removing unwanted dissociation pro- ducts, and SF_6 is becoming increasingly used in high power circuit breakers where it is purged after current interruption and restored at 200 psi.

In choosing a high pressure gas insulant, other factors than electrical strength, toxicity and cost can be significant. Heat transfer can be an important characteristic, and where there is moving equipment the influence of gas density on windage has to be considered. The electric strength of a gas usually increases with its den- sity, but there is also a dependence on molecular structure. It has been shown experimentally that the larger the molecular cross section, the higher is the dielectric strength.[32] Whereas SF_6 has a dielectric strength of 2.5 relative to nitrogen, SeF_6 has a relative strength of 4.5; but is toxic. Sharbaugh and Watson[33] have studied the per- fluorocarbon vapor(FC-75) which is liquid at room temperatures, and mixtures of the vapor with SF_6. At 100°C with FC-75 in the presence of SF_6 the breakdown strength was almost 100% above that of SF_6 alone.

It has already been noted that coating the negative electrode of a vacuum gap with a suitable dielectric, can improve breakdown strength; pre- sumably by the suppression of field emission. McNeall and Skipper[34] have shown that at 250 psig of N_2 the uniform field impulse breakdown stress can be increased by more than 50% when the cathode is covered with a 0.005 inch layer of polyethylene. The improvement, however, is lost after one breakdown because of puncture of the dielectric layer. In the d.c. case, it seems that although a dielectric film on the cathode sur- face decreases conditioning activity, it does not improve the ultimate voltage holding properties.[35]

The flash-over strength of solid dielectrics in gases increases almost linearly with pressure. Reyes[36] has obtained flash-over voltages for sev- eral materials immersed in equal parts of CO_2 and N_2 at 350 psi (Fig. 9), and has shown that breakdown voltage could be increased very signi- ficantly by corrugating the dielectric surface.

In designing for high pressure insulation it is usual to assume that breakdown will occur at a critical field. For example, in a Van de Graaff accelerator which has a coaxial geometry, the field on the inner conductor is considered criti- cal. Such machines can operate at 19 MV / m

in N_2 and CO_2 mixtures at 300 psig. Michael, et al[37] have designed and operated an accelerator with a stress of 25 MV/m on the terminal using 10% SF_6 and 90% N_2 at 250 psig. Pure SF_6 at 150 psia has supported more than 40 MV/m inside a pressure to vacuum feedthrough bushing.[16]

4. Two Unusual Accelerators

With the current interest in space technology a need has developed for accelerators of small micrometeoroid sized particles. Specifically, a machine is being developed[38] for the acceleration to velocities approaching 10^5 m/sec of micron size particles having charge to mass ratios in the range 10 to 10^3 coulombs per kilogram. The relatively low velocity of these massive particles, which makes traveling electromagnetic field methods of acceleration impracticable, facilitates the simple acceleration concept shown in Fig. 10.

The particle source used in this accelerator was developed by Vedder.[39] A single particle is suspended electrodynamically in a high vacuum and charged positively by ion bombardment prior to injection into the accelerator system. The particle is then accelerated into the first equipotential cylinder, which in this machine is at 500 kV negative. The cylinder is crowbarred to ground by the spark gap before the particle emerges from the far side, so that a further energy gain of 500 kV can be obtained in the field between the first and second cylinders; and so on.

The accelerating electrodes in this first machine are supplied by individual Van de Graaff generators because of uncertainties about supply interactions, but machines having many stages probably would require only one supply and a gas insulated transmission line carrying potential to each of the electrodes which would have r.f. isolation from the line.[40]

The high voltage pressure to vacuum bushing uses SF_6 at 150 psia to insulate the central conductor where it passes through the ground plane, and the glass dielectric surface of the bushing on both the high pressure side ($N_2 + CO_2$) and the high vacuum side is voltage graded by a semiconducting plastic.[16] The problem of sequencing the several crowbars is not difficult because the particles are within each cylinder for several microseconds. The several components of this accelerator have been largely checked out, and the complete system will be operating shortly.

Flash X-ray machines have for some time been used for the radiography of small fast moving objects, but there is a present need for fast radiography at a distance, and for the simulation of radiation from nuclear weapons, which has led to the development of new, more powerful pulsed radiation sources. The approach described below is undoubtedly the simplest, and is proving most effective.

The concept is outlined in Fig. 11. A coaxial gas capacitor, which is essentially the elongated terminal of a Van de Graaff generator and the surrounding pressure tank, is charged to several megavolts then discharged at the open end into the load by a fast spark gap switch. The length of the coaxial capacitor is chosen to give the desired pulse duration, which in nanoseconds is twice the terminal length in feet.

There are four major elements in the system. One is the voltage generator, which has been developed to beyond 10 MV in the form of the Van de Graaff machine. Its characteristics are not significant to the discharging (transient) properties of the system, except that the stored energy in the column adds slightly to the tail of the radiation pulse. The other major elements are the coaxial gas capacitor, the triggered megavolt switch, and the load, which is a field emission accelerator tube. The switch will not be discussed further here beyond noting that a high pressure, high gradient spark switch, with a suitable trigatron type geometry, is sufficiently fast and closes with a delay less than 10 nanoseconds. The important feature of the machine, which is the pulsed emission tube and its interaction with the coaxial line, is discussed briefly below.

First it is necessary to note the output characteristics of a transmission line charged to a voltage V_o which is discharged into a load R (assumed resistive). A primary pulse of voltage amplitude $V = \alpha V_o$, current amplitude $I = V/R$ and duration 2τ is produced, where

$$\alpha = \frac{R}{R + Z_o} \qquad (1)$$

Z_o = characteristic impedance of the line, and

τ = the electrical length of the line.

For a coaxial line with a dielectric constant of 1, the electrical length is approximately 1 nanosecond per foot of length, and

$$Z_o = 60 \ln \frac{r_2}{r_1} = \sqrt{\frac{L}{C}} \qquad (2)$$

where r_2, r_1 are respectively the outer and inner radii of the coaxial cylinders and L, C are the inductance and capacitance per unit length of the line.

Maximum power is transferred into the load when $R = Z_o$, but from expression (1) it can be seen that this is when $V = V_o/2$. The requirement here is not for maximum power transfer, but for the maximum radiation intensity produced by an accelerated electron beam, which varies roughly with the third power of the voltage. At this point it is necessary to examine how a transmission line will perform when discharged into a field emission load.

The upper plot on Fig. 12 shows a typical current/voltage relationship for a field emission gap. An excellent review of the field emission process and its potentialities is given by Dyke.[41] The minimum field geometry in a coaxial gas capacitor is when $\ln r_2/r_1 = 1$ or $Z_o = 60\Omega$, and the lower plot on Fig. 12 shows for a specific charging voltage the load characteristic of a transmission line with that impedance. A replot of the field emission characteristic is also given. The intersection of the two curves is the operating point, with the transmission line developing a pulsed voltage corresponding to a load $R = V/I$ at the operating point. There is no time delay between field emission and applied field, at least in the time regime of interest here, which with the above argument implies that the field emission tube can be treated as a resistive load R on the line as determined above. Actually, during the pulse when there are high currents flowing the tube impedance will fall somewhat because of changes in the field emission characteristic.

It is now possible to relate the characteristics of the coaxial line to the ultimate requirement - namely radiation intensity. It can easily be shown from information in Reference 42, that the radiation intensity (R_I) produced by an electron beam accelerated to a voltage V at 12" from a gold target in the forward direction is given by

$$R_I = 3.72 \times 10^6 \times I \times V^{3.4} \text{R/s at 12"} \qquad (3)$$

where V is the voltage in megavolts and I is the current in kiloamperes.

Noting the relationship between V and I for the coaxial line, it follows that

$$R_I = \frac{3.72 \times 10^9 (1 - \alpha) \alpha^{3.4} V_o^{4.4}}{Z_o} \qquad (4)$$

Differentiating to determine α for maximum R_I for V_o and Z_o constant gives

$$\alpha = \frac{3.4}{4.4} = 0.775 \qquad (5)$$

The maximum intensity at 12" from the target is then given by

$$R_I = \frac{0.353 \times 10^9 \times V_o^{4.4}}{Z_o} \text{R/s} \qquad (6)$$

This expression shows the very strong dependence of radiation intensity on charging voltage V_o, which is determined by the radial dimensions of the coaxial line. For the 60Ω (minimum field) geometry the maximum charging voltage is given by $E_c r_1$ where E_c is the critical field. Some values of critical field in a high pressure gas have been given earlier in this paper. With a charging voltage of 5.5 MV, intensities approaching 10^{10} R/s at 12" would be produced based on the above expressions. Actually in a system designed for multishot performance, a broad anode spot has to be used to maintain target integrity and the intensity would be less than that given by expression (6), although the radiation field would be more uniform.

A prototype FX machine in horizontal configuration is shown in Fig. 13. This machine was made by modifying an existing Van de Graaff generator equipped with an extra long tank for testing accelerator tubes. Although not originally designed as a flash X-ray machine, it is operating well and producing 20 nanosecond pulses of 2 R at 1 meter. This corresponds to an electron beam current of 19 kiloamperes at 2.3MeV. Several pulses of radiation can be delivered per minute, and there is essentially no electromagnetic noise problem because the high power transients are contained within a closed metal shell. The present terminal structure is rather crude, and with improvements the machine is expected to develop 5×10^9 R/s (100 R) at 12". A larger machine designed specifically for flash X-ray is under construction.

Acknowledgement

References

1. Disruptive Breakdown Measurements of Solid Materials in a Non-Uniform D. C. Field, R. C. Charpentier, Paper No. 29, 33rd Annual Conference on Electrical Insulation, (October, 1964).

2. R. Elcox, Ion Physics Corporation, Private Communication.

3. Electron Emission in Intense Electric Fields, R. H. Fowler and L. Nordheim, Proc. Roy. Soc. (London) A119, 173, (1928).

   The Effect of the Image Force on the Emission and Reflexion of Electrons by Metals, L. Nordheim, ibid, A121, 626, (1928).

4. Field Emission and Its Influence on Breakdown in Vacuum, C. N. Coenraads. Paper presented at 24th Annual Conference on Physical Electronics, (March, 1964)--see also Reference 9.

5. Vacuum Breakdown for Broad Area Tungsten Electrodes, D. Alpert, D. A. Lee, E. M. Lyman, and H. E. Tomaschke, Proc. Sym. on Insulation of High Voltages in Vacuum, (October, 1964), p. 1.

6. Initiation of Electrical Breakdown in Ultra-high Vacuum, D. Alpert, D. A. Lee, E. M. Lyman, and H. E. Tomaschke, Jour. of Vacuum Science and Technology, 1, 35, (1964).

7. Field Emission Initiated Vacuum Arc, W. P. Dyke, J. K. Trolan, E. E. Martin, and J. P. Barbour, Phys. Rev. 91, 1043, (1953).

8. Electrical Breakdown in High Vacuum, W. S. Boyle, P. Kisliuk, and L. M. Germer, Jour. Appl. Phys. 26, 720, (1955).

9. Some Effects of Electrode Metallurgy and Field Emission on High Voltage Insulation Strength in Vacuum, F. McCoy, C. N. Coenraads, and M. Thayer, Proc. Sym. on Insulation of High Voltages in Vacuum, (October, 1964) - Addendum.

10. Measurements on a High-Gradient Accelerating Tube Model, J. Huguenin and R. Dubois, Proc. Sym. on Insulation of High Voltages in Vacuum (October, 1964)

11. Pre-breakdown Conduction Between Electrodes in Continuously-Pumped Vacuum Systems, W. K. Mansfield and R. L. Fortescue, Brit. J. Appl. Phys. 8, 73, (1957).

12. Electric Microdischarges in Dynamic Vacuum, R. Arnal, Ann. Physik 12, 830, (1955) in French; USAEC-TR-2837, English Trans.

13. Prebreakdown Conduction Between Electrodes in Ultra-High and High Vacuum, L. I. Pivovar and V. I. Gordienko, Sov. Phys.-Tech. Phys. 7, 908, (1963).

14. The Characteristics of the Vacuum Spark, A. S. Denholm, Ph. D. Thesis, Univ. of Glasgow, (1955).

15. The Initiation of Electrical Breakdown in Vacuum, L. Cranberg, J. Appl. Phys. 23, 518, (1952).

16. Ability of a Voltage-Graded Surface to Support a High Voltage in Vacuum and in a Pressurized Gas, R. B. Britton, K. W. Arnold and A. S. Denholm, R.S.I. 34, 185, (1963).

17. Pre-breakdown Conduction in Continuously-Pumped Vacuum Systems, W. K. Mansfield, Brit. J. Appl. Phys. 11, 454, (1960).

18. Microdischarges and Predischarge Between Metal Electrodes in High Vacuum, R. I. Pivovar and V. I. Gordienko, Sov. Phys. - Tech. Phys. 28, 2101, (1958).

19. The Sources of Electron-Induced Contamination in Kinetic Vacuum Systems, A. Ennos, Brit. J. Appl. Phys. 5, 27, (1954).

20. Properties of Inclined-Field Acceleration Tubes, K. H. Purser, A. Galejs, P. H. Rose, R. J. Van de Graaff and A. Wittkower. Proc. Sym. on Insulation of High Voltages in Vacuum (October, 1964) p. 317.

21. Electrostatic Power Generator - Final Technical Report on Contract AF33(615)-1168, Air Force Aero Propulsion Laboratory, RTD, Wright-Patterson AFB, Ohio (1965).

22. Vacuum Insulation of High Voltages Utilizing Dielectric Coated Electrodes, L. Jedynak, Jour. Appl. Phys. 35, 1727, (1964).

23. Some Studies on High Voltage Vacuum Break-down Across Large Gaps. Investigation of the Properties of Oxide-Coated Aluminum Electrodes, F. Rohrbach, Proc. Sym. on Insulation of High Voltages in Vacuum, (October, 1964) p. 393.

24. Electrical Breakdown over Insulators in High Vacuum, P.H. Gleichauf, Jour. Appl. Phys. 22, 535 and 766, (1951).

25. Effect of Metal-Dielectric Junction Phenomena on High Voltage Breakdown over Insulators in Vacuum, AIEE Trans. III, 79, 999, 1960.

26. Insulation of High Voltage Across Solid Insulators in Vacuum, J.P. Shannon, S.F. Philp, and J. G. Trump, Proc. Sym. on Insulation of High Voltages in Vacuum (October, 1964) p. 281.

27. The Effect of the Presence of an Oxide-Coated Cathode on the Voltage Insulation of Nickel Electrodes in High Vacuum, I. Brodie, ibid, p. 237.

28. Influence of Electrodes on D.C. Breakdown in Gases at High Pressure, J. G. Trump, R. W. Cloud, J. G. Mann and E. P. Hanson, Elec. Eng. 69, 961, 1950.

29. Compressed Gas Insulation in the Million-Volt Range: A Comparison of SF_6 with N_2 and CO_2, S. F. Philp, AIEE Trans. on Power Apparatus and Systems, No. 66, 356, (1963).

30. Insulation Properties of Compressed Electro-Negative Gases, P. R. Howard, Proc. IEE 104, A, 132, (1957).

31. Electric Strength of Highly Compressed Gases, E.M. Cohen, Proc. IEE, 103, A, (1956).

32. Electric Strength and Molecular Structure of Saturated Gaseous Hydrocarbons, R. W. Crowe, J. C. Devins, Annual Report, Conf. on Electrical Insulation, N.R.C. (1953).

33. Breakdown Strengths of a Perfluorocarbon Vapor (FC-75) and Mixtures of the Vapor with SF_6, A.M. Sharbaugh and P.K. Watson, IEE Trans. on Power Apparatus and Systems, No. 2, 131, (1964).

34. The Impulse Flashover Strength of Solid Insulators in Compressed Gas, P.I. McNeall and D. J. Skipper, Proc. Int. Conf. Gas Discharges and the Electricity Supply Industry, (May, 1962) Butterworths, London.

35. R. C. Charpentier, High Voltage Engineering Corporation, Private Communication.

36. High Voltage Breakdown Studies on Solid Dielectrics, R. A. Reyes, S.M. Thesis, Electrical Engineering, MIT, (1960).

37. New Electrostatic Accelerator, I. Michael, E. D. Berners, F.J. Eppling, D.J. Knecht, L. C. Northcliffe and R. G. Herb, RSI 30, 855, (1959).

38. A Preliminary Design Study of a Microparticle Accelerator, Final Report-Contract NAS2-1873, Ion Physics Corporation, (April, 1964).

39. Charging and Acceleration of Microparticles, J. F. Vedder, RSI 34, 1175, (1963).

40. R. N. Cheever, Ion Physics Corporation, Private Communication.

41. Advances in Field Emission, W.P. Dyke, Scientific American, 210, 108, January, 1964.

42. Radiographic Properties of X-Rays in the Two-to-Six Million-Volt Range, C.H. Goldie, K.A. Wright, J. H. Ansen, R.W. Cloud and J. G. Trump, ASTM Bulletin No. 201, 49, (October, 1954).

Table 1

Breakdown Strengths of Film at 293°K, 77°K, 4°K

Material	Temp. °K	MV/in	δ%	Tests
Kodar Polyester (3/4 mil)	293	9.35	20	5
	77	10.3	15	5
	4	11.1	10.8	5
Mylar Polyester (2 mils)	293	10.45	11.6	5
	77	7.58	2.46	6
	4	7.12	3.8	4
FEP Teflon (9.9 mils)	293	9.95	6.8	4
	77	3.3	11.5	5
Lexan Polycarbonate (4.5 mils)	293	15.1	5.13	5
	77	5.65	11.7	6
	4	5.9	19	3
Polyethylene (commercial) (2 mils)	293	10.25	10	6
	77	11.3	15.8	7
	4	1.35	25	5
Polyethylene (9.5 mils)	293	6.4	4.8	3
	77	3.24	5.6	5
	4	1.54	3.1	3
H-Film Polyimide (1 mil)	293	7.36	7.17	5
	77	10.8	5.2	5
	4	10.8	2.3	5

Table 2

Relative Contamination Caused by Vacuum Materials
(t = 100 min, $I = 0.01$ A/cm^2, $V = 2$ kV)

Material	Treatment	Thickness of Contamination Deposit(Å)
Diffusion pump oil (Apiezon B)	As supplied	1700
Silicone diffusion pump oil (Dow-Corning 703)	As supplied	500
Vacuum grease (Apiezon M)	As supplied	1500
Apiezon W Wax (cold)	As supplied	< 50
Black neoprene (heavily loaded to give oil resistance)	Boiled in aqueous and alcoholic potash	< 50
O-ring rubber gasket material (W. Edwards and Co., Ltd., London)	Boiled in aqueous and alcoholic potash	600
Brass strip*	Well handled and not subsequently cleaned	700
Brass strip	Cleaned in acid	< 50
Aluminum strip*	Well handled and not subsequently cleaned	700
Aluminum strip	Cleaned in aqueous potash	< 50

* Area of metal equal to internal surface area of electron gun.
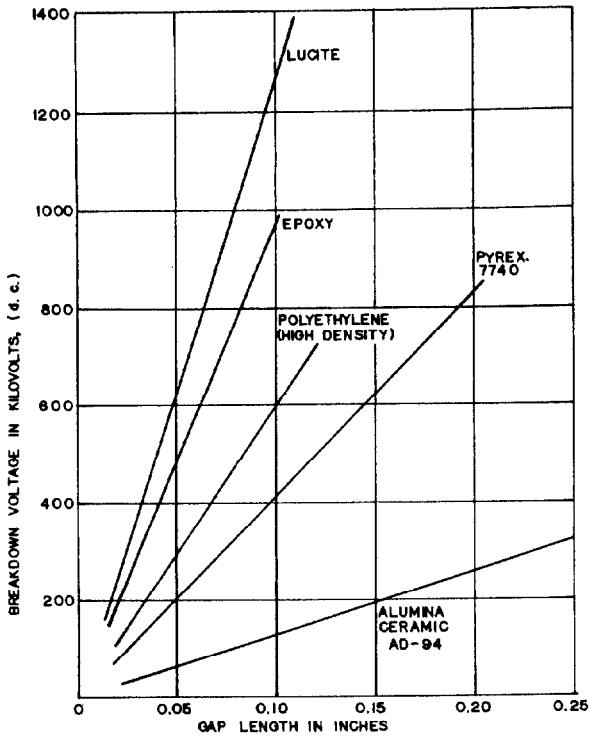
Fig. 1. Disruptive Breakdown Voltage
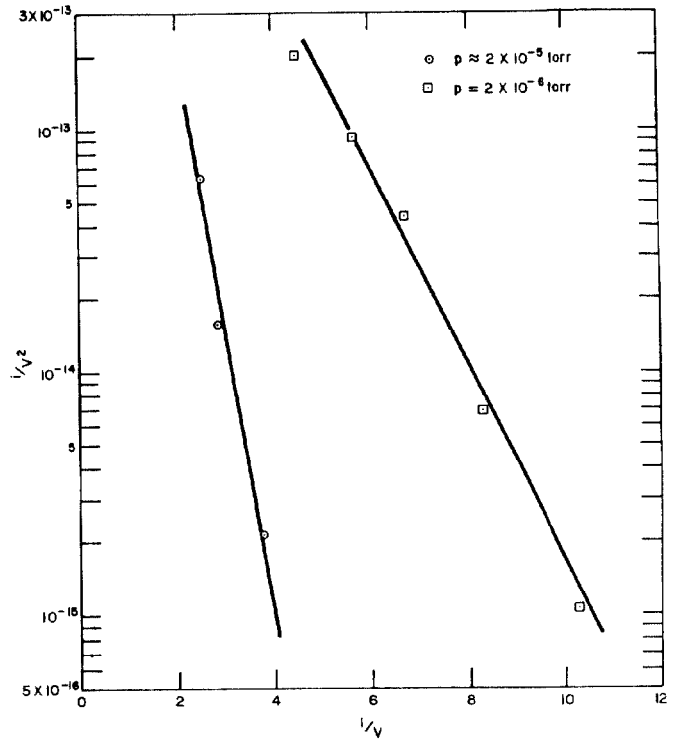for Solid Dielectrics.

Fig. 2. Fowler-Nordheim Plot
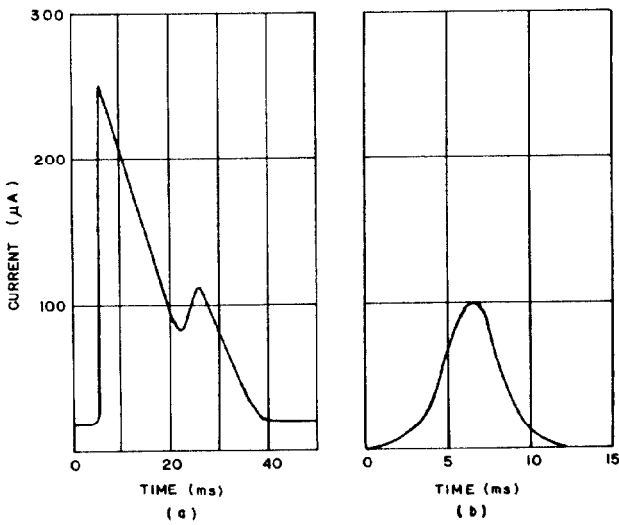for 304 Stainless Steel Emitter.

Fig. 3. Microdischarge Pulses
(Mansfield and Fortescue[11]).
(a) Waveform of Pulse occurring
between copper electrodes with
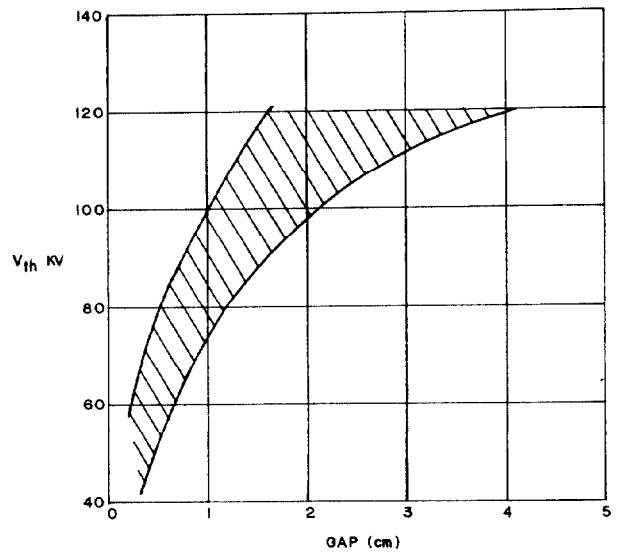a 1 cm gap. (b) Waveform of
pulse for accelerator tube.

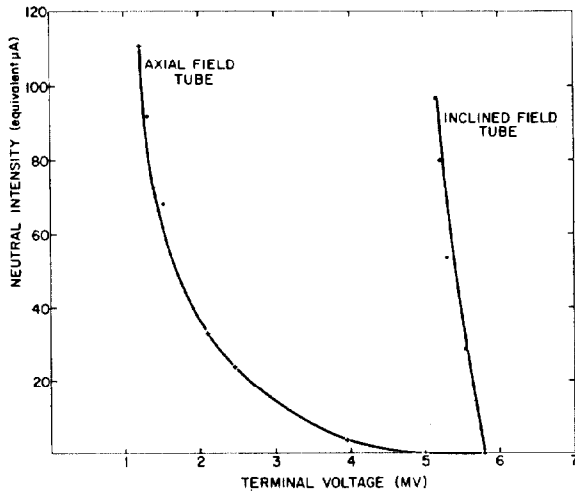Fig. 4. Range of Threshold Voltages
for Microdischarges (Arnal[12]).

Fig. 5. The Reduction in Terminal Voltage
as a Function of Injected Neutral Beam
Intensity for a Constant Charging Current.
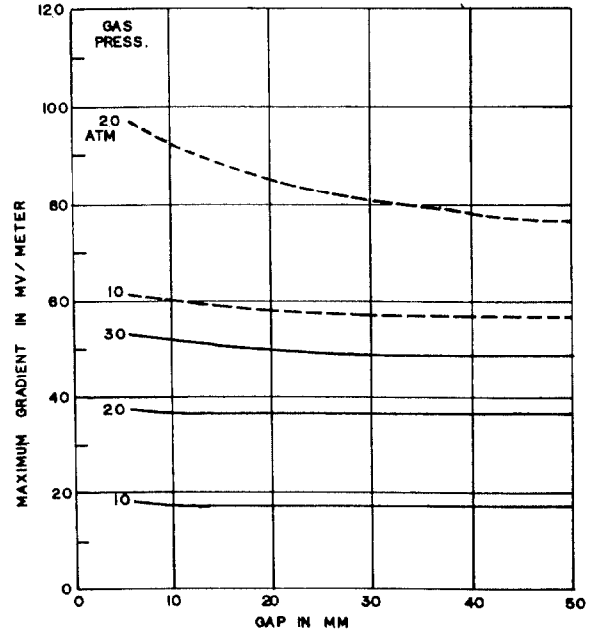
Fig. 7: Maximum Gradients on 64-mm Spheres
Facing Negative High-Voltage Terminal in
SF_6 (Broken Lines) and N_2 + CO_2 (Solid lines).
Curves are given for various values of
gas pressure.
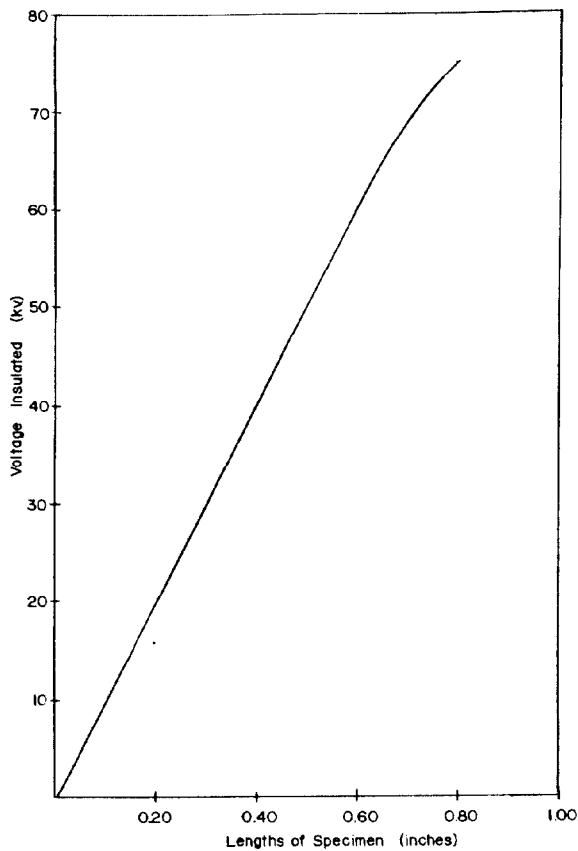
Fig. 6. Insulation Strengths Over
Al_2O_3 Surfaces in Vacuum.
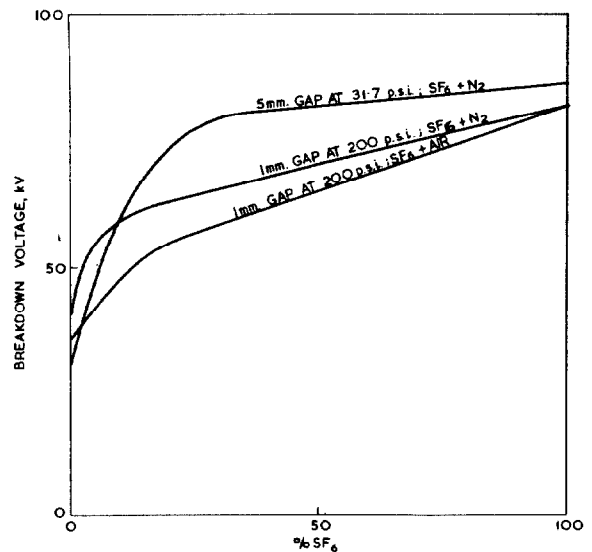
Fig. 8. Dependence of Breakdown Voltage on SF_6
Content for Mixtures of SF_6 and Air and Nitrogen.
The abscissa is the partial pressure of SF_6 ex-
pressed as a percentage of the total pressure of
the mixture from data by Howard[30] and Cohen[31].
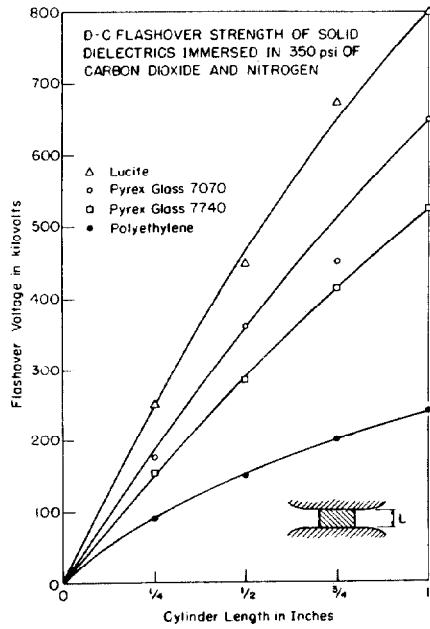
Fig. 9. D-C Flashover Strength of Solid Dielectrics
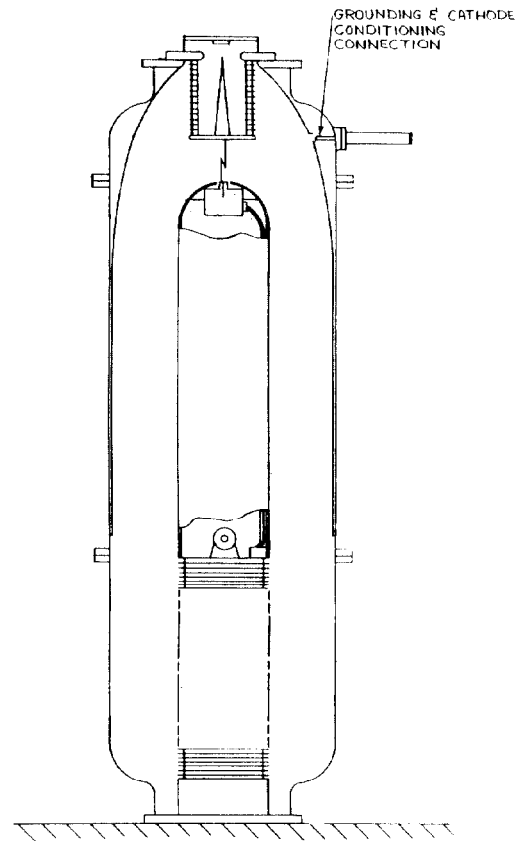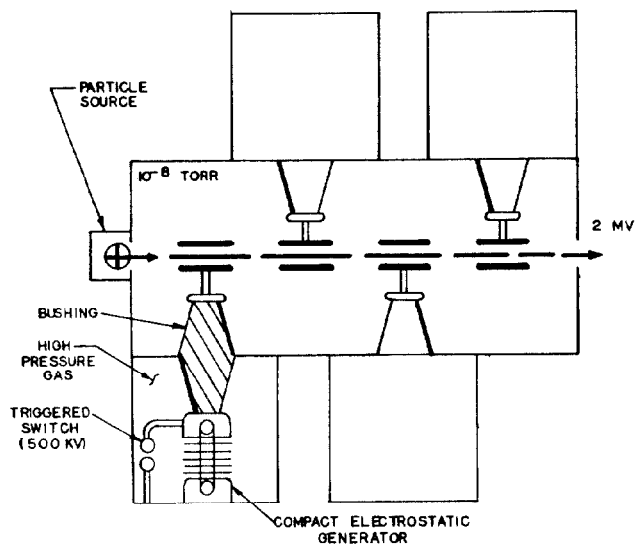Immersed in 350 psi of Carbon Dioxide and Nitrogen.

Fig. 10. Heavy Particle Linear Accelerator Concept.

Fig. 11. Outline of Coaxial Pulses Machine.

Fig. 13. FX 1 Machine with Charging Column and line Withdrawn.
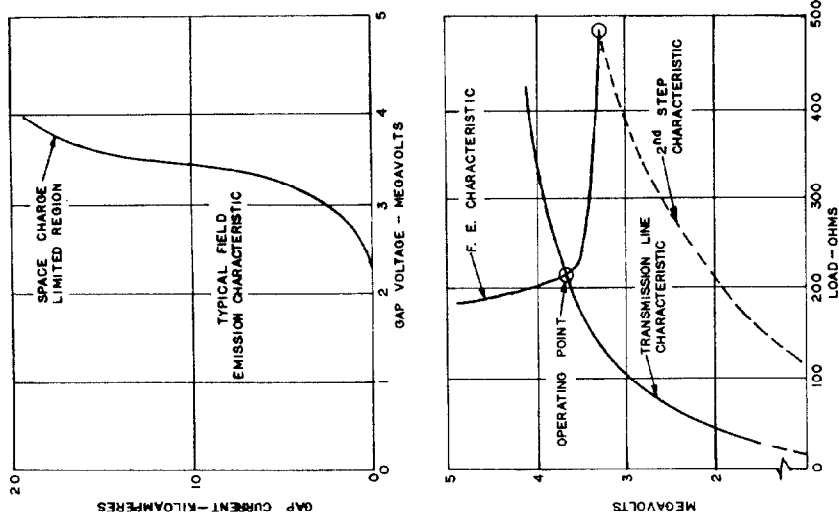
Fig. 12. Derivation of Field Emission Tube Operating Point.